Geological Survey of Japan Cruise Report No, 21, p. 219-230, 1986

XIV. MINERALOGY AND INTERNAL STRUCTURE OF MANGANESE NODULES IN THE GH81-4 AREA

Akira Usui

Introduction

Normal deep-sea manganese nodules are composed of limited members of ferromanganese minerals, despite quite variable morphology and bulk chemical composition. Principal mineral constituents of these nodules are 10 Å manganate and δ-MnO_2 (2-line form), and some silicate minerals. Our earlier numerous mineralogical investigations in the Central Pacific Basin have proved that 10 Å manganate and δ-MnO_2 represent rough surface and smooth surface of nodules respectively, and that relative abundance of the two minerals principally determines bulk chemical compositions of nodules (USUI *et al.*, 1978; USUI and MOCHIZUKI, 1982). It is because each mineral is of distinct and rather constant chemical composition, and represents characteristic microstructures (USUI, 1979). These differences and other on-site occurrences on/in sediments are interpreted that each mineral is formed through different supply routes; 10 Å manganate is formed through diagenetic remobilization of metals during diagenesis of unconsolidated sediments, and δ-MnO_2 is formed through direct supply of metals from overlying normal sea water (USUI *et al.*, 1978). Mineralogical characteristics are therefore most important in characterizing deep-sea manganese nodules and in considering nodule growth processes.

Bulk X-ray diffraction analysis and chemical analysis of the nodules were carried out for the same powder sample of each station. Diffraction analyses were made during GH81-4 cruise on board and after the cruise. Several split nodules were prepared for microscopical observation on polished sections.

Methods of determination of manganese minerals

Mineralogy of marine manganese minerals is still controversial as summarized by BURNS and BURNS (1977, 1979) and ARRHENIUS *et al.* (1979). In this article following mineral terms are tentatively adopted after some modification from ARRHENIUS *et al.* (1979); 10 Å manganate (comparable to terrestrial *todorokite*), 7 Å manganate (comparable to terrestrial *birnessite*), and δ-MnO_2 (restricted to 2-line form). These minerals are identifiable on diffractograms and their relative abundances in each powder sample were semi-quantitatively determined. All X-ray diffraction analyses were accomplished in the constant measurement conditions using the diffractometer Type RAD-rA (Rigaku Denki Co. Ltd.) with a monochromator. Powder samples mounted in standard glass holders were subjected to nickel-filtered Cu radiation at 40 kV and 160 mA during 8° (2θ)/min scan from 3° to 45° (2θ). Peak heights at six d-spacings were measured to estimate these manganese minerals. 10 and 5 Å reflections are diagnostic of 10 Å manganate, 7 and 3.5 Å reflections of 7 Å manganate, and 2.4 and 1.4 Å reflections are responsible to the above two minerals and δ-MnO_2. Typical X-ray

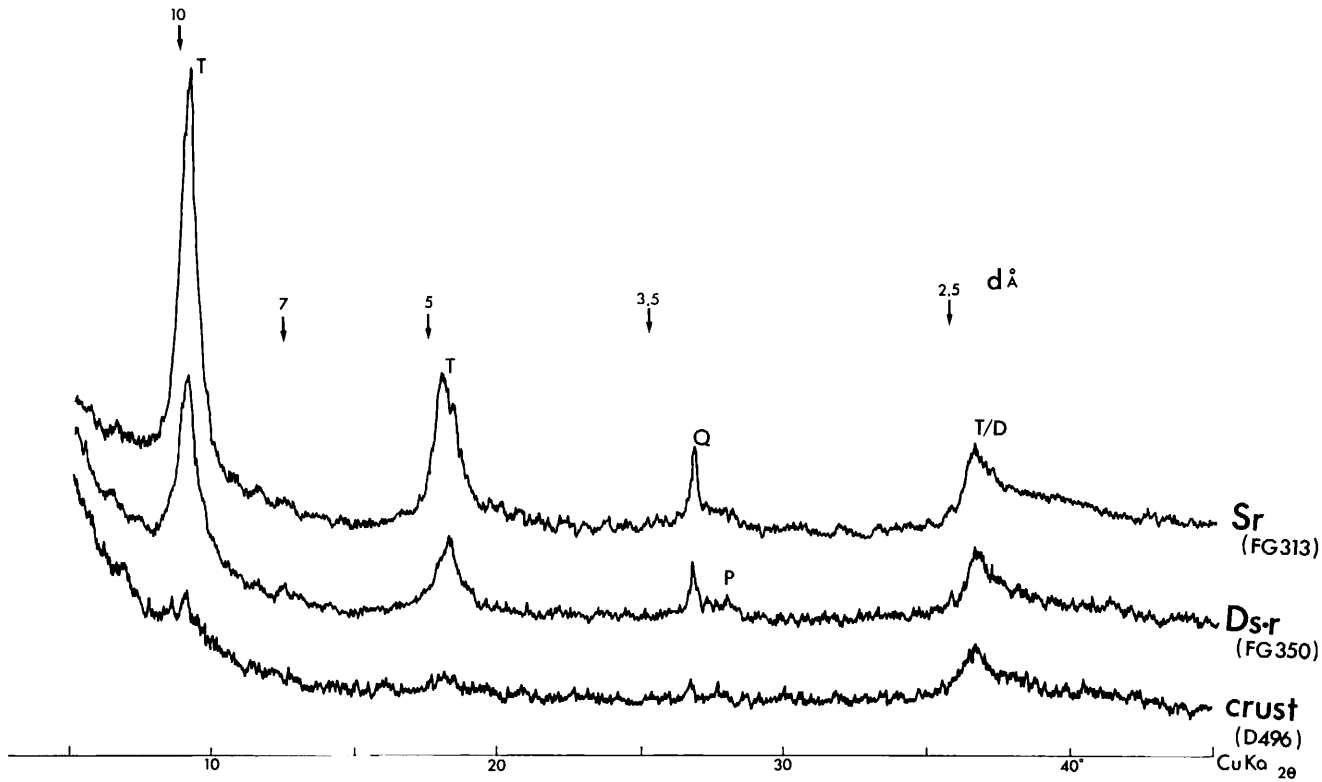

Fig. XIV-1 Typical X-ray powder diffraction patterns of manganese nodules from the GH81-4 area. Manganese mineral abundance varies with nodule morphology. T: 10 Å manganate, D: δ-MnO_2 (2 line form), Q: quartz, P: plagioclase.

Table XIV-1 Criteria of optical determination of manganese minerals under reflecting microscope for the Central Pacific Basin nodules (after USUI, 1979).

Minerals	10 Å manganate	δ-MnO_2
Color	light grey	dark grey
Reflectivity (560 nm)	high (ca. 13%)	low (ca. 8%)
Anisotropism	strong	none
Hardness (VHN*)	high (55-112, mean 82)	low (10-24, mean 17)
Internal reflection	none	none

*Vicker's hardness number.

powder diffraction patterns are shown in Fig. XIV-1.

Approximate abundance of these minerals were estimated on the basis of rounded X-ray intensity values. That of δ-MnO_2 was calculated from the intensities at 10 and 2.4 Å d-spacings assuming that the intensity ratio of pure 10 Å manganate is 5.0, as the peaks of two minerals overlap at 2.4 Å d-spacing. Accessory silicate minerals, quartz, feldspars, clay mineral zeolites, and apatites were examined in terms of ASTM data files.

Microscopic identification of manganese minerals is based on earlier works. 10 Å manganate and δ-MnO_2 phases are distinguishable on polished sections according to the criteria for optical determination by USUI (1979) as shown in Table XIV-1.

X-ray diffraction analysis of manganese nodules

The X-ray diffraction study shows that 10 Å manganate and 2 line form δ-MnO_2 are principal manganese minerals of the nodules from the GH81-4 area, though the former is dominant. 7 Å reflections responsible to manganese minerals were not detected except for only one sample from the piston core P218. These occurrences of manganese minerals are consistent with our earlier works in the Central Pacific Basin (USUI, 1984 and others) and in the northeastern equatorial Pacific (PIPER *et al.*, 1977). Results of analyses for GH81-4 nodules are listed as approximate abundances in Table XIV-2. Analysis numbers in the table are common to those for chemical analyses in Table XV-1.

To examine the relationships between nodule morphology and mineral composition, powder samples were taken so as to represent the mean characteristics of nodules within individual stations. Morphology of these nodules is variable around abyssal hills, but little difference was observed between nodule tops and bottoms. The compositions of manganese minerals are closely related to nodule morphology (Table XIV-2) as revealed in earlier works (MORITANI *et al.*, 1977; Usui and MOCHIZUKI, 1982). Smooth surfaces are always composed or the δ-MnO_2 while rough surfaces of 10 Å manganate. However, bulk mineral compositions are not always consistent with nodule types, because manganese mineral composition is sometimes variable from nodule surface to interior (e.g., FG368, FG381).

Manganese-free accessory minerals determined in the nodules of this study are quartz, plagioclase, phillipsite, and smectite. These silicate minerals may be incorporated into nodules as fine particles and/or nuclei. Quartz is commonly incorporated into almost all samples and shows two- to three-fold variation. The quartz content

Table XIV-2 Mineral abundance in manganese nodules of the GH81-4 area.

No.	Station	Sample	Type	Mineral abundanece							Area	Remarks
				T	S	D	Qz	Ph	Pc	Mnt		
1	2577	FG313	R2	xxx	-	+	x	-	-	-	I	one nodule
2	2578	FG314	R2	xxx	-	+	x	xx	x	-	I	one nodule
3	2579	P218	-	xxx	xx	+	-	-	-	-	I	pipe (32cm depth)
4		P218	-	xx	xxx	xx	-	-	-	-	I	cusps(32cm depth)
5		P218	-	xxx	-	x	-	+	+	+	I	plate(32cm depth)
6		FG315	R2	xxx	-	+	x	-	x	-	I	2 nods.
7	2580	FG322-1	I2	xx	-	+	+	x	-	-	-	one nodule
8		-2	I2	xx	-	x	+	-	-	-	-	one nodule
9	2581	FG311	R2	xxx	-	+	x	-	-	-	-	one nodule
10	2582	FG312	R2	xxx	-	+	x	-	-	-	I	2 nods.
11	2583	P220	R2	xx	-	x	x	xx	x	x	I	one nodule(core top)
12		FG327	R2	xxx	-	+	+	-	-	-	I	4 nods.
13	2588	FG317	R2	xxx	-	+	+	-	-	-	I	half a nodule
14	2594	FG316-1	R2	xxx	-	+	x	-	-	-	-	2 nods.
15		-2	R1	xx	-	x	+	-	-	-	-	2 nods.
16	2596	FG342	R2	xxx	-	+	x	-	-	-	-	2 nods.
17	2597	FG341-1	R2	xxx	-	+	+	-	-	-	-	3 nods.
18		-2	R2	xxx	-	+	x	-	-	-	-	one nodule
19	2598	FG329	R2	xxx	-	+	x	-	-	-	-	2 nods.
20	2605	FG335	R1	xx	-	x	+	-	-	-	II	one nodule
21	2606	FG334	R2	xxx	-	+	x	-	-	-	II	3 nods.
22	2608	FG338	R2	xxx	-	+	x	-	-	-	II	3 nods.
23	2609	FG343	R2	xxx	-	+	x	-	-	-	I	2 nods.
24	2610	FG344	R2	xxx	-	+	x	-	-	-	I	2 nods.
25	2611	FG345	R2	xxx	-	+	x	-	-	-	I	one nodule
26	2617	FG350	I1	xx	-	x	+	-	-	-	I	one nodule
27	2619	FG351	R2	xxx	-	+	x	-	-	-	I	3 nods.
28	2620	FG352	R2	xxx	-	+	x	-	-	-	I	3 nods.
29	2621	FG353	S1	x	-	xx	+	-	+	-	I	2 nods.
30	2622	B59	S1	x	-	xx	+	-	-	-	I	2 nods.(core top)
31	2624	FG355	R2	xxx	-	+	+	-	-	-	I	3 nods.
32	2625	FG356	R2	xxx	-	+	+	-	-	-	I	3 nods.
33	2626	FG357	R2	xxx	-	+	+	-	-	-	I	4 nods.
34	2627	FG358	R2	xxx	-	+	+	-	-	-	I	2 nods.
35	2628	B60	R2	xxx	-	+	+	-	-	-	I	2 nods.(core top)
36			R2	xxx	-	+	+	-	-	-	I	2 nods.(core top)
37	2630	FG360	R2	xxx	-	+	+	-	-	-	I	2 nods.
38	2631	FG361	R2	xxx	-	+	x	-	-	-	I	2 nods.
39	2632	FG362	S1	x	-	xx	+	-	-	-	I	2 nods.
40	2633	FG363	S1	+	-	xx	-	xx	-	-	I	2 nods.
41	2634	B61	S1	x	-	xx	-	xx	-	x	I	2 nods.(core top)
42	2635	FG364	S1	x	-	x	+	x	-	x	I	2 nods.
43	2636	FG365	R2	xxx	-	+	x	-	-	-	I	2 nods.
44	2637	FG366	R2	xxx	-	+	x	-	+	-	I	4 nods.
45	2638	FG367	R2	xxx	-	+	x	-	-	-	I	3 nods.
46	2640	FG368	S2	xx	-	+	+	-	-	-	I	2 nods.
47	2641	FG369	R2	xxx	-	+	+	-	-	-	I	half/ 4cm dia.
48			R2	xxx	-	+	x	-	-	-	I	2 nods./ 2.5 cm dia.
49			R2	xxx	-	+	x	-	-	-	I	4 nods./ 1-2 cm dia.
50			R2	xxx	-	+	x	-	-	-	I	7 nods./ 0.5 cm dia.
51	2642	FG370	R2	xxx	-	+	x	-	-	-	I	2 nods.
52	2644	FG372	R2	xxx	-	+	x	-	-	-	I	2 nods.
53	2645	B63	S1	+	-	xx	+	-	-	x	I	2 nods.(15 cm depth)
54			S1	+	-	xx	+	-	-	x	I	2 nods.(15 cm depth)
55	2646	FG373	R1	xx	-	x	x	-	-	-	I	2 nods.
56	2647	FG374	R1	x	-	x	+	-	-	-	I	one nodule
57	2648	FG375	R2	xxx	-	+	+	-	-	-	I	2 nods.
58	2649	FG376	R2	xxx	-	+	x	-	-	-	I	2 nods.
59	2650	FG377	I1	xx	-	x	+	xx	-	x	I	2 nods.
60	2651	P224	I2	xx	-	+	+	-	-	-	I	one nodule(core top)
61	2652	FG378	S1	x	-	xx	+	xx	-	+	I	2 nods.

Table XIV-2 (continued)

No.	Station	Sample	Type	Mineral abundanece						Area	Remarks
				T	S	D	Qz	Ph	Pc	Mmt		
62	2653	FG379	S1	x	-	xx	+	xx	-	x	I	one nodule
63	2654	FG380	S1	x	-	xx	+	-	-	-	I	one nodule
64	2655	FG381	I2	xxx	-	+	x	-	-	-	I	2 nods.
65	2656	FG382	R2	xxx	-	+	x	-	-	-	I	3 nods.
66	2657	B64	R2	xxx	-	+	x	+	-	-	I	3 nods.(core top)
67	2659	FG384	S1	+	-	xx	+	-	-	-	I	1/4 nods.
68	2660	FG385	I1	x	-	+	+	-	-	-	I	half a nodule
69	2661	FG386	I2	xxx	-	+	x	-	-	-	I	2 nods.
70	2662	FG387	R2	xxx	-	+	x	-	-	-	I	2 nods.
71	2663	P225	R2	xx	-	x	+	-	-	-	I	1/4 nods.(core top)
72	2666	FG390	R2	xxx	-	+	x	-	-	-	I	2 nods.
73	2667	FG391	R2	xxx	-	+	x	-	-	-	I	2 nods.
74	2668	FG392	R2	xxx	-	+	x	-	-	-	I	3 nods.
75	2669	B65	R2	xxx	-	+	x	-	-	-	I	one nodule/1.5cm(core top)
76			R2	xxx	-	+	x	-	-	-	I	3 nods./0.5-1cm dia.(do.)
77			R2	xxx	-	x	x	-	+	-	I	25nods./0.5cm (do.)
78	2670	FG424	R2	xxx	-	+	x	-	-	-	I	half a nodule/3cm dia.
79			R2	xxx	-	+	x	-	-	-	I	2 nods./1.5 cm dia.
80			R2	xxx	-	+	x	-	-	-	I	3 nods./1 cm dia.
81			R2	xxx	-	+	xx	-	+	x	I	5 nods./ 0.5 cm dia.
82			R2	xxx	-	+	x	-	-	x	I	4 nods.
83	2671	FG426	R2	xxx	-	+	xx	-	-	x	I	2 nods.
84	2677	FG394	R2	xxx	-	+	x	-	-	-	II	3 nods.
85	2678	FG395	R2	xxx	-	+	x	-	-	-	II	3 nods.
86	2679	FG396	R2	xxx	-	+	x	-	-	-	II	one nodule
87	2680	FG397	R2	xxx	-	+	x	-	-	-	II	one nodule
88	2681	B66	R2	xxx	-	+	x	-	-	-	II	2 nods.(core top)
89	2684	FG400	R2	xxx	-	+	x	-	-	-	II	3 nods.
90	2686	FG402	R2	xx	-	+	x	-	-	-	II	2 nods.
91	2687	FG403	R2	xx	-	x	x	x	-	-	II	2 nods.
92	2690	FG405	R2	xxx	-	+	xx	-	-	-	II	2 nods.
93	2691	FG407	I1	xx	-	x	+	x	-	x	II	2 nods.
94	2693	FG408	R2	xxx	-	+	+	-	-	-	II	3 nods.
95	2695	B67	R1	xx	-	+	x	-	-	x	II	one nodule(core top)
96	2696	FG410	R2	xxx	-	+	x	-	-	-	II	2 nods.
97	2698	FG412	R2	xxx	-	+	x	-	-	-	II	one nodule
98	2699	FG413	R2	xxx	-	+	x	-	-	-	II	2 nods.
99	2705	B68	R2	xx	-	x	xx	-	-	-	II	2 nods.(core top)
100	2706	FG418	R2	xxx	-	+	x	-	-	-	II	3 nods.
101	2710	FG422	R2	xxx	-	+	x	-	-	-	II	2 nods.
102	2711	FG423	I1	xx	-	x	+	-	-	x	II	half a nodule
103	2712	P229	R1	xx	-	x	+	x	-	-	II	one nodule(core top)
104	2713	D496	-	+	-	xx	-	-	-	-	I	crust/ 1cm thick
105			S1	xx	-	xx	+	-	+	-	I	one nodule
106			R2	xxx	-	+	+	+	-	-	I	1/4 nods./ 5cm dia.
107			R2	xxx	-	+	x	-	-	-	I	4 nods. /1.5cm dia.
108	2635	FG364	R2	xx	-	x	x	-	-	-	I	3 nods.

Sample no. / FG:free-fall grab, B:box corer, P:piston corer.
Nodule type / R1: type r of irregular shape, R2: type r of spherical or discoidal shape, S1: type s of irregular shape, S2:type s of spherical shape, I1: intermeditate type of irregular shape, I2: intermeditate type of spherical or discoidial shape.
Mineral species / T: 10 Å manganate, S: 7 Å manganate, D: δ-MnO_2, Qz: Quartz, Ph: phillipsite, Pc:plagioclase, Mmt: montmorillonite.
Mineral abundance/ XXX: very abundant, XX: abundant, X: present, +: tranceable, -: not detected.

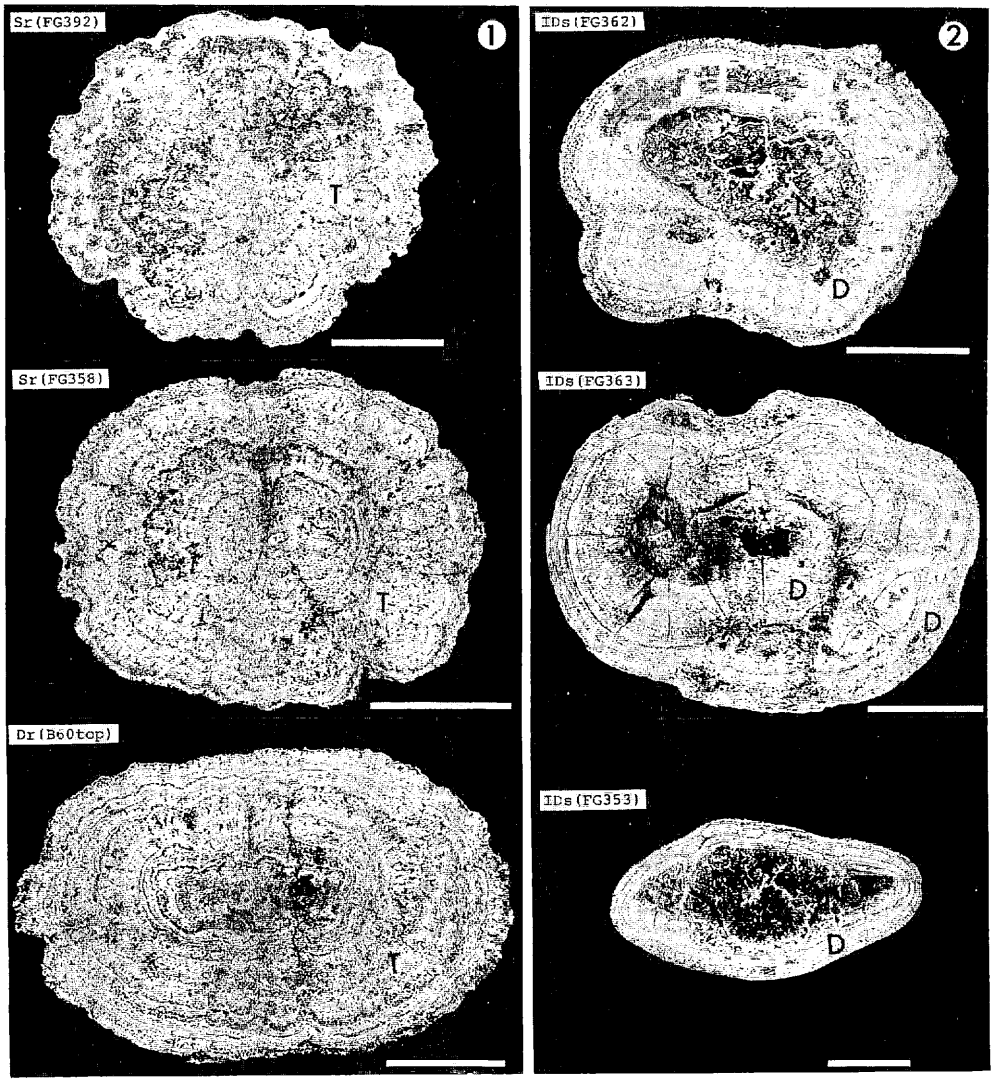

Fig. XIV-2(1)

Fig. XIV-2 Photographs of cross section of manganese nodules taken under reflecting lights, showing typical internal structure patterns. Morphology (S: spherical, D: discoidal, I: irregular, P: polynucleated, s: smooth surface, r: rough surface) and sample number (in parenthesis) are on the upper left corner of each photo. Mineral composition of internal layers are symbolized on photos (T: 10 Å manganate, D: δ-MnO_2, N: nuclei). Scale bar: 1 cm.

does not appear to vary with nodule type or manganese mineral composition. Phillipsite seems to be associated with s-type nodules. It may be attributable mostly to frequent occurrence of zeolitic claystone as nodule nuclei or included fragments. Smectite also seems to be associated with the claystone.

Local variation of internal structure of nodules around abyssal hills

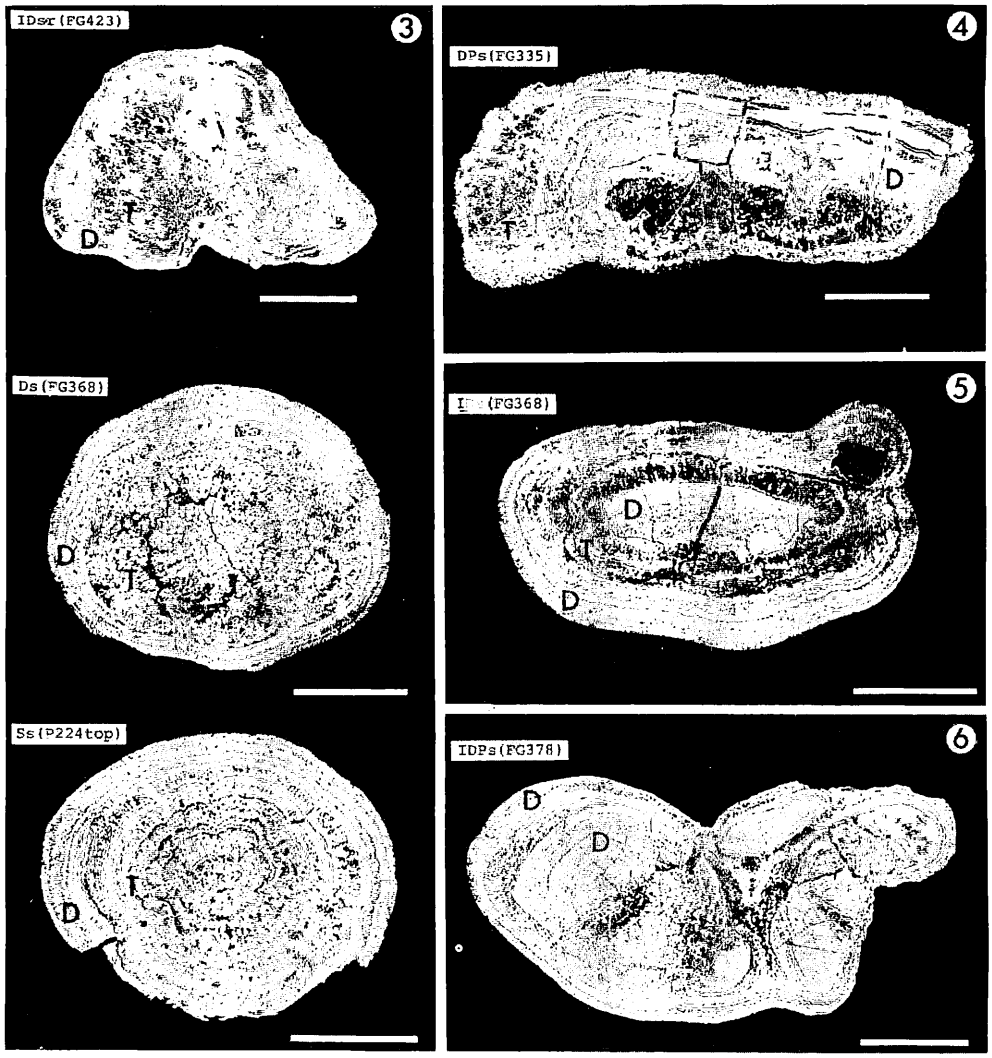

Fig. XIV-2(2)

Internal structure of nodules were described by means of megascopic and microscopic observations. Nodules of this area also consist of two ferromanganese minerals. The two principal mineral phases, which form characteristic microstructure respectively, could be employed as stratigraphic units of nodules. Three phases were defined under microscope according to optical properties (USUI, 1984) as follows:

(1) 10 Å manganate phase: cuspate or dendritic growth structure composing rough surface of nodules,

(2) δ-MnO_2 phase: monotonic stratified or massive structure composing smooth surface of nodules,

(3) fine microscopic alternations of the above two phases, sometimes showing intermediate features of nodule surface.

Nodules from all stations were stratigraphically examined under reflecting

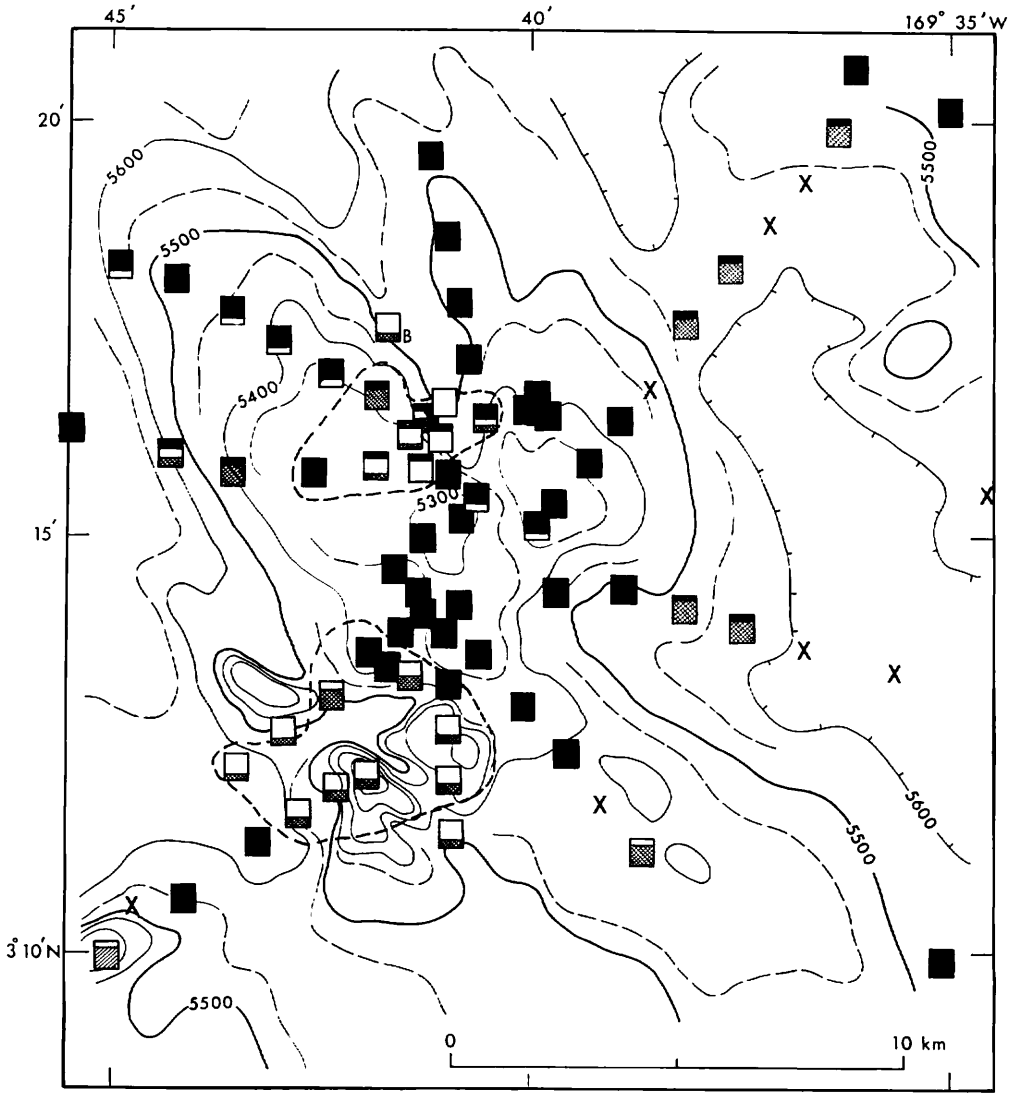

Fig. XIV-3 Local variation of nodule internal structure in the detailed survey area I. Dashed lines: sea floor coverage of nodules greater than 5%.

microscope in terms of above simplified mineralogical method. Nodules frequently include conformable and unconformable boundaries between the phases. These boundaries are the results of sequential or intermittent growths of nodules. Typical patterns of internal nodule stratigraphy are shown in Fig. XIV-2 as follows:

1) nodules entirely composed of 10 Å manganate (T), 2) nodules entirely composed of δ-MnO_2 (D) occasionally with uncontinuous growth layers and large nuclei, 3) type s including type r inside, 4) type r of irregular shape including a fragment of type s, 5) complicated structure suggesting a change of surface feature from smooth to rough

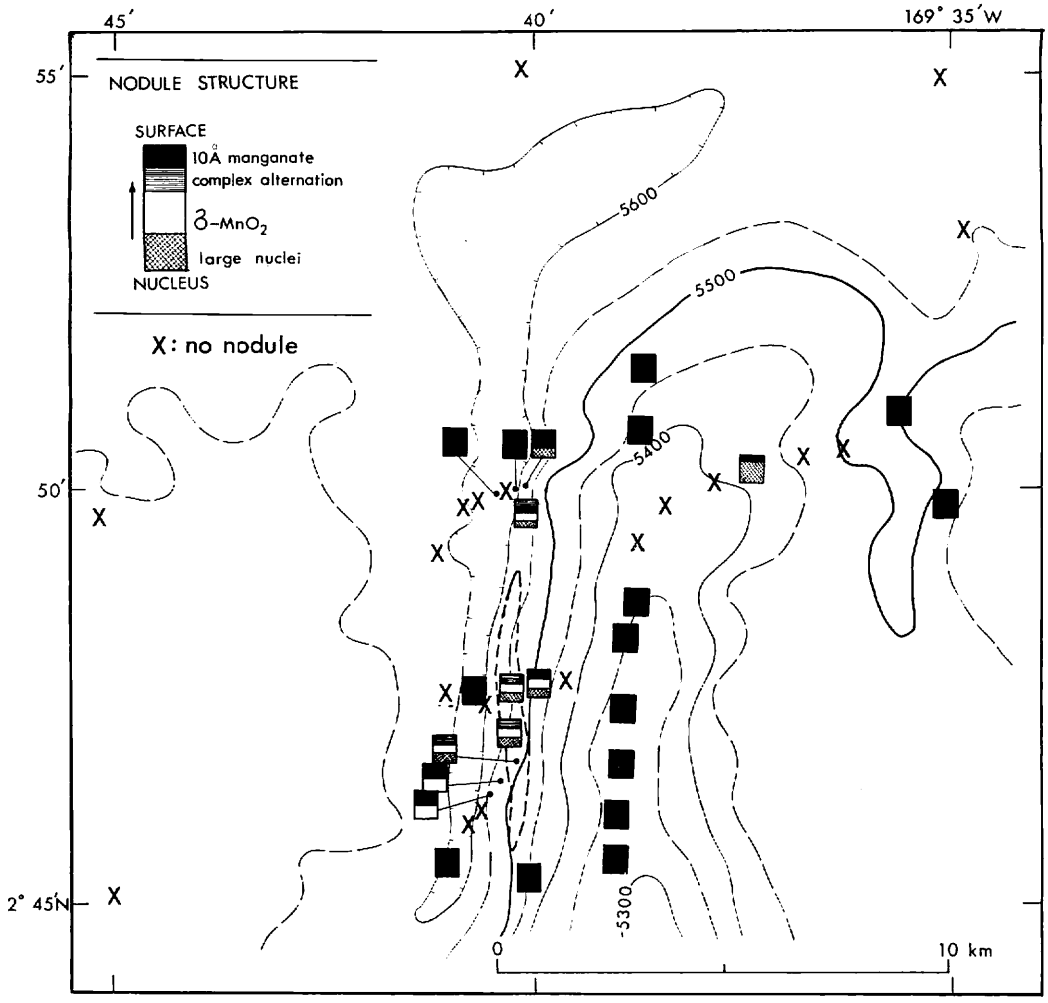

Fig. XIV-4 Local variation of nodule internal structure in the detailed survey area II. Dashed lines: sea floor coverage of nodules greater than 5%.

and smooth during its growth, 6) type s including older nodule fragments of type s.

Figures XIV-3 and -4 show small-scale variations of nodule internal structures. Both in the detailed survey areas I and II, internal structure, as well as surface structure, is variable near the hill tops and the flanks. As shown in these figures, the pattern of local variations of nodule internal structure has no distinct relation to topography or water depths. Acoustic stratigraphy of sediments (USUI and TANAHASHI, this cruise report) appear to be related to nodule internal structure. The r-type nodules having simple concentric structure tend to occur with the uppermost transparent layers both on the hill tops and in the basin areas. The s-type nodules entirely composed of δ-MnO_2 and those including δ-MnO_2 nodules inside, are preferentially distributed in the area of outcrop of the older opaque layers. Especially, complicated internal structures

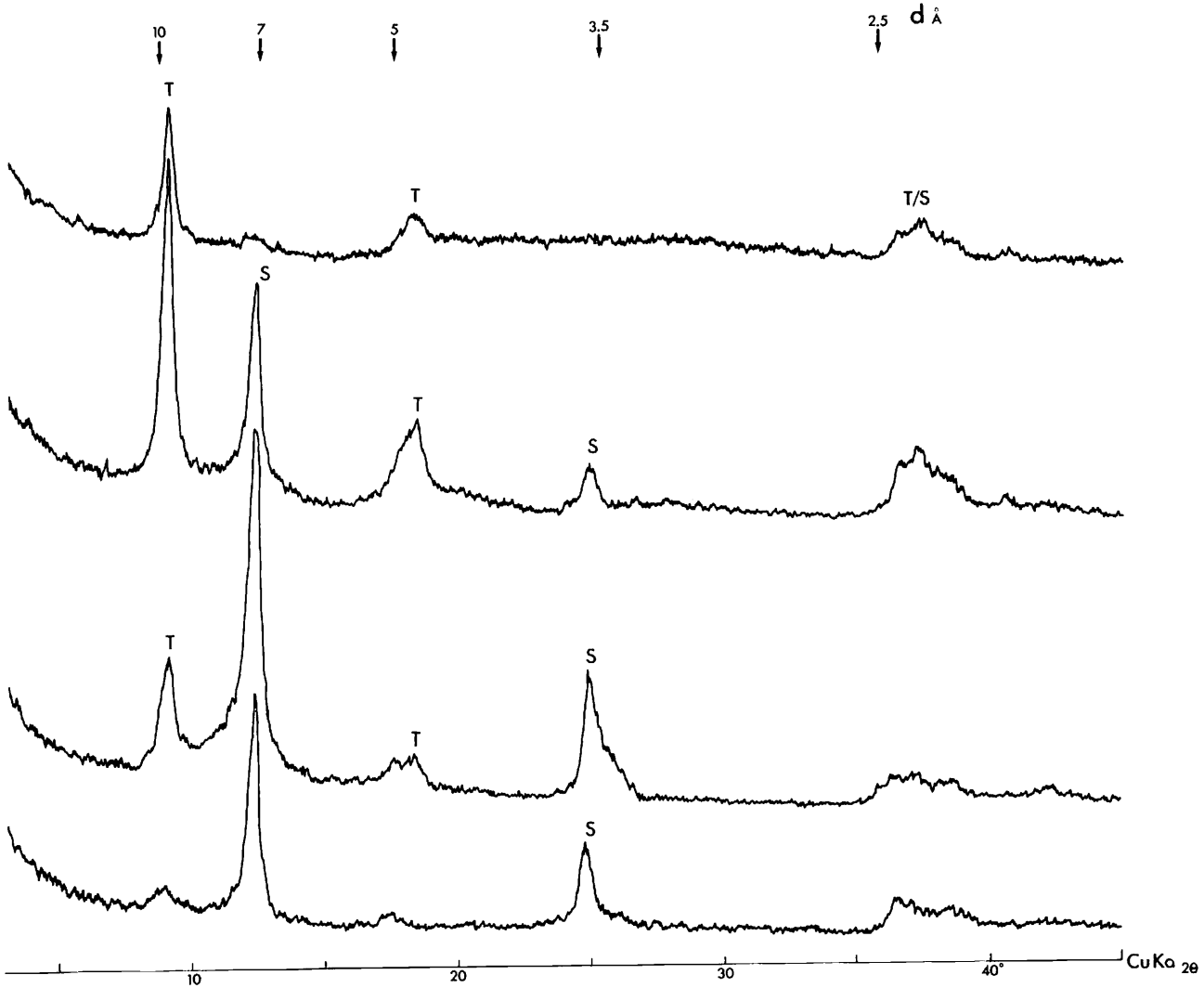

Fig. XIV-5 X-ray powder diffraction patterns of manganese concretions from P218. All powder samples were taken out of one concretion. T: 10 Å manganate, S: 7 Å manganate.

are encountered around the boundary between the areas of the transparent layers and the outcrop.

These tendencies in relation to acoustic stratigraphy suggest an optimal development of δ-MnO_2 under a condition of no or slow sedimentation and a genetical relationship of 10 Å manganate to sedimentation of siliceous sediments composing transparent layers. However, the studies of nodule growth rates and ages are needed to verify the optimal sedimentary conditions for nodule growth.

Manganese oxide concretions from piston core P218

Irregular shaped (pipes, rods, dendrites, and plates) manganese concretions were collected between depths 30 to 35 cm from the sea floor within the piston core P218. On-board and in-laboratory X-ray diffraction analyses reveal that these materials are composed of very pure manganese oxides, 10 Å manganate and 7 Å manganate. As shown in Fig. XIV-5, four characteristic d-spacings (10, 7, 5, and 3.5 Å) are not from one mineral, because two of the diagnostic peak sets inversely vary in several powder samples from one concretion. They contain traceable amounts of Fe, Si, and Al, and little transition metals (USUI and TERASHIMA, this cruise report). The pipe-, rod-, and dendrite-shaped concretions show metallic luster, and may be fine mixtures of the two manganese minerals. The plate-shaped concretion is earthy black, and may be an aggregate of manganese micronodules of 10 Å manganate.

Occurrence of 7 Å manganate (comparable to terrestrial birnessite) in deep-sea manganese nodules is very rare, but reported from nodules in the caldera of a young seamount (LONSDALE *et al.*, 1980) and from manganese micronodules in pelagic sediments (GLOVER, 1977). Abnormal chemical and mineral compositions of the P218 manganese concretions suggests that they are of different origin from normal deep-sea manganese oxide minerals. The chemical composition is similar to that manganese nodules diagenetically formed in shallow water environments (BONATTI *et al.*, 1972), and the mineral composition is similar to those of hydrothermal origin from active mid-oceanic ridges (CRONAN *et al.*, 1982). Further chemical and mineralogical investigations in relation to associated sediment cores are needed before we conclude the origin of these concretions.

References

ARRHENIUS, G., CHEUNG, K., CRANE, L., FISK, M., FRAZER, J., KORKISCH, J., MELLIN, T., NAKAO, S., TSAI, A. and WOLF., G. (1979) Counterions in marine manganates. *In* LALOU, C. (ed.), *Colloques Internationaux du* C. N. R. S. No. 289, *La Genèse des Nodules de Manganèse*, p. 333-356.

BONATTI, E., HONNOREZ, J., JOENSUU, O. and RYDELL, H. (1972) Classification and genesis of submarine iron-manganese deposits. *In*: D. R. HORN (ed.) *Ferromanganese Deposits on the Ocean Floor*. NSF, Washington D. C., p. 149-166.

BURNS, R. G. and BURNS, V. M. (1977) Mineralogy of mananese nodules. *In*. G. P. BURNS (ed.), *Marine Manganese Deposits*, Elsevier Publ. Co., New York, p. 185-248.

BURNS, R. G. and BURNS, V. M. (1979) Manganese oxides. *In* R. G. BURNS (ed.) *Marine Minerals*, Mineral. Soc. America Short Course Notes, vol. 6., p. 1–46.

CRONAN, D. S. (1977) Deep-sea nodules: Distribution and geochemistry. *In* G. P. GLASBY (ed.) *Marine Manganese Deposits*. Elsevier Publ. Co., New York, p. 11–44.

GLOVER, E. D. (1977) Characterization of marine birnessite. *Am. Mineral.*, vol. 62, p. 278–285.

LONSDALE, P., BURNS, V. M. and FISK, M. (1980) Nodules of hydrothermal birnessite in the caldera of a young seamount. *J. Geol.*, vol. 88, p. 611–618.

MORITANI, T., MARUYAMA, S., NOHARA, M., MATSUMOTO, K., OGITSU, T. and MORIWAKI, H. (1977) Description, classification, and distribution of manganese nodules. *Geol. Surv. Japan Cruise Report*, no. 8, p. 136–158.

PIPER, D. Z., CANNON, W. and LEONG, K. (1979) Composition and abundance of ferromanganese nodules at DOMES Sites A, B, and C: Relationship with bathymetry and stratigraphy. *In* PIPER D. Z. *et al.* (eds.), *Deep Ocean Environmental Study: Geology and Geochemistry of DOMES Sites A, B, and C, Equatorial North Pacific*, USGS Open-file Rept. 77–778, p. 217–266.

USUI, A. (1979) Minerals, metal contents and mechanism of formation of manganese nodules from the Central Pacific Basin (GH76–1 and GH77–1 areas). In: BISCHOFF, J. L. and PIPER, D. Z. (Eds.), *Marine Geology and Oceanography of the Pacific Manganese Nodule Province*, Plenum, New York, p. 651–677.

——— (1984) Mineralogy and internal structure of manganese nodules of the GH80–5 area. *Geol. Surv. Japan Cruise Rept.*, no. 19, in press.

——— and MOCHIZUKI, T. (1982) Regional variation of manganese nodule chemistry from Wake to Tahiti, GH80–1 cruise. *Geol. Surv. Japan Cruise Report*, no. 18, p. 338–354.

———, SHOJI, T. and TAKENOUCHI, S. (1978) Mineralogy of deep sea manganese nodules and synthesis of manganese oxides: Implications to genesis and geochemistry. *Mining Geology*, vol. 28, p. 405–420.